

# Specification Requirements for a Combined Dehumidifier/Cooling Panel: A Global Scale Analysis

Damien Gondre, Hatem Ben Maad, Abdelkrim Trabelsi, Frédéric Kuznik, Joseph Virgone

**Abstract**—The use of a radiant cooling solution would enable to lower cooling needs which is of great interest when the demand is initially high (hot climate). But, radiant systems are not naturally compatibles with humid climates since a low-temperature surface leads to condensation risks as soon as the surface temperature is close to or lower than the dew point temperature. A radiant cooling system combined to a dehumidification system would enable to remove humidity for the space, thereby lowering the dew point temperature. The humidity removal needs to be especially effective near the cooled surface. This requirement could be fulfilled by a system using a single desiccant fluid for the removal of both excessive heat and moisture. This task aims at providing an estimation of the specification requirements of such system in terms of cooling power and dehumidification rate required to fulfill comfort issues and to prevent any condensation risk on the cool panel surface. The present paper develops a preliminary study on the specification requirements, performances and behavior of a combined dehumidifier/cooling ceiling panel for different operating conditions. This study has been carried using the TRNSYS software which allows nodal calculations of thermal systems. It consists of the dynamic modeling of heat and vapor balances of a 5m x 3m x 2.7m office space. In a first design estimation, this room is equipped with an ideal heating, cooling, humidification and dehumidification system so that the room temperature is always maintained in between 21°C and 25°C with a relative humidity in between 40% and 60%. The room is also equipped with a ventilation system that includes a heat recovery heat exchanger and another heat exchanger connected to a heat sink. Main results show that the system should be designed to meet a cooling power of  $42\text{W}\cdot\text{m}^{-2}$  and a desiccant rate of  $45\text{ g}_{\text{H}_2\text{O}}\cdot\text{h}^{-1}$ . In a second time, a parametric study of comfort issues and system performances has been achieved on a more realistic system (that includes a chilled ceiling) under different operating conditions. It enables an estimation of an acceptable range of operating conditions. This preliminary study is intended to provide useful information for the system design.

**Keywords**—Dehumidification, nodal calculation, radiant cooling panel, system sizing.

## I. INTRODUCTION

THE control of indoor humidity especially in hot and humid climates represents in recent years one of the major fundamental problems which must be treated to maintain human comfort and ensure building durability [1], [2]. The conventional vapor compression refrigeration cycles used in commercial air conditioners consume large amount of electricity due to important thermal losses: generally, in such regions, the thermal insulation is of bad quality. The

production of electricity in these countries is also considered as a difficulty in summer season. Alternative solar and desiccant coolers technologies have greater potential and great advantages of improving thermal comfort. Radiant cooling system combined with liquid desiccant dehumidification is a relatively good candidate [3].

Compared with the conventional vapor-compression cooling dehumidification systems, sensible and latent cooling load are decoupled and controlled separately, which means that control of humidity can be achieved better [4]. Coupled with a porous membrane, the liquid desiccant dehumidification system removes heat and moisture from the air. Membranes can also improve absorptive and evaporative processes, which are used in technologies like absorption chillers, liquid desiccant dehumidifiers, and evaporative coolers; technologies that are energy efficient. However, the risk of condensation on the cooling dehumidification surfaces represents a significant problem when the surface temperature is close to or lower than the dew point temperature [5]. The temperature of the liquid has to be controlled to avoid this problem, which is made using a sink source at moderate level (water from the sea for example).

The aim of the present study is thus intended to provide estimations of the maximum cooling power and the maximum dehumidification rate required to meet comfort requirements while avoiding condensation risks. In fact, the purpose of this work is to assess how much humidity and heat is to be removed from the office space but not to assess how it will be done. At this development stage, a global scale analysis which calculates heat and moisture balances of a typical office space seems to be sufficient. The scope of the study will thus be limited to the office space with its ventilation system. It will not be taken into account the desiccant fluid neither the regeneration loop, as shown in Fig. 1.

## II. DESCRIPTION OF THE SIMPLIFIED MODEL

### A. Presentation of the System

Fig. 1 shows how a combined radiant cooling/dehumidification system could work.

**Ventilation.** The indoor air (1) renewal is achieved with a mechanical ventilation system. Inlet fresh air is pre-cooled with a heat recovery exchanger and cooled down with a second heat exchanger connected to a heat sink. The nature of the heat sink is not detailed yet, but it could take advantage of ground inertia (geothermal energy) or water inertia, or could be an electrically powered sink such as a heat pump. Based on the first design, it seems that the ventilation system only uses sensible heat exchangers. The inlet fresh air that is blown in

D. Gondre, H. Ben Mâad, A. Trabelsi, F. Kuznik, and J. Virgone are with the Univ Lyon, CNRS, INSA-Lyon, Université Claude Bernard Lyon 1, CETHIL UMR5008, F-69621, Villeurbanne, France (e-mail: damien.gondre@insalieu.org, hatem.ben-maad@univ-lyon1.fr, abdelkrim.trabelsi@univ-lyon1.fr, frederic.kuznik@insa-lyon.fr, joseph.virgone@univ-lyon1.fr).

the space thus arrives with the same absolute humidity of outside conditions, unless condensation occurs (in which case air is blown at saturated humidity).

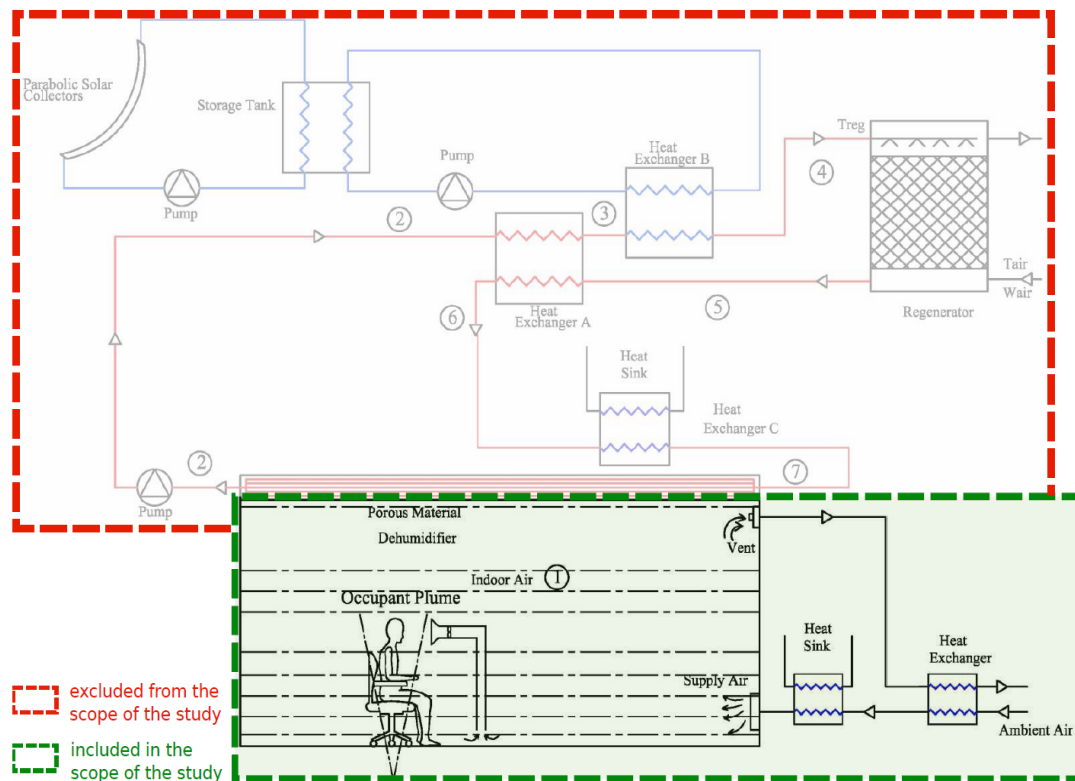


Fig. 1 Sketch of the full system showing what is included and what is not included in the simplified modeling

**Ceiling panel.** Additional cooling needs are provided by the ceiling panel in which a saturated and cold desiccant fluid flows in (7). The desiccant fluid is channeled by a porous membrane that prevents any liquid leaks in the office space while enabling vapor transfer across its surface. Since the desiccant fluid is saturated, it shows a high affinity for water molecules and tends to dry the indoor air (1) near the membrane surface.

A mass transfer of water molecules occurs from the indoor air to the desiccant fluid through a mechanism involving convection (in the air), diffusion (in the membrane) and absorption (in the desiccant fluid). Please note that the absorption mechanism releases heat inside the desiccant fluid, lowering its cooling power.

**Regeneration loop.** The desiccant fluid is warmer and less saturated at the outlet of the ceiling panel (2). It then calls for a regeneration system that intends to remove water molecules from the desiccant fluid in a regenerator. The fluid is solar heated in a heat exchanger (B) prior to be sprayed in the regenerator surfaces (4) where ambient air evaporates water molecules. A hot and dry desiccant fluid then comes out of the regenerator (5) prior to be cooled down successively by a heat recovery exchanger (A) (6) and a heat sink exchanger (7).

### B. Methodology

This study is developed on the Trnsys 17 simulation

software [6]. A 3D description of the office space is used so that the influence of radiation can be accounted for in a detailed calculation way (using view factors).

A 5m\*3m\*2.7m office space is drawn with the Trnsys 3d plug-in for Google Sketch Up (Fig. 2). The south oriented wall is external. The floor is adjacent to the ground. The ceiling is adjacent to a plenum space which is adjacent to the roof. All other surfaces are partition walls adjacent to other rooms (and thereby considered as adiabatic). Wall layouts and material properties used in the simulation are summed up in Tables II and III.

The study is split into three steps, with different levels of complexity and different objectives as summed up in Table I and described here under.

**Step 1:**Free evolution. Estimate temperature and humidity values under a free evolution in order to highlight the need of a thermo-hygro regulation.

**Step 2:**Ideal HVAC systems. Estimate required dehumidification rate and cooling power in order to instantly fulfill temperature and humidity set points.

**Step 3:**Realistic system. Implement a chilled ceiling and find its best operating conditions (in terms of inlet temperature and maximum flowrate) to fulfill system performance and comfort issues.

TABLE I  
CHARACTERISTICS OF EACH OF THE THREE SIMULATION STEPS CONSIDERED  
IN THE STUDY

|                         | STEP 1<br>Free<br>EVOLUTION | STEP 2<br>IDEAL<br>SYSTEMS   | STEP 3<br>RADIANT<br>COOLING |
|-------------------------|-----------------------------|------------------------------|------------------------------|
| <b>Ventilation</b>      | Direct                      | Heat recovery<br>+ Heat sink |                              |
| <b>Heating</b>          | None                        | Ideal                        | Ideal                        |
| <b>Cooling</b>          | None                        | Ideal                        | Ceiling panel                |
| <b>Humidity control</b> | None                        | Ideal                        | Ideal                        |

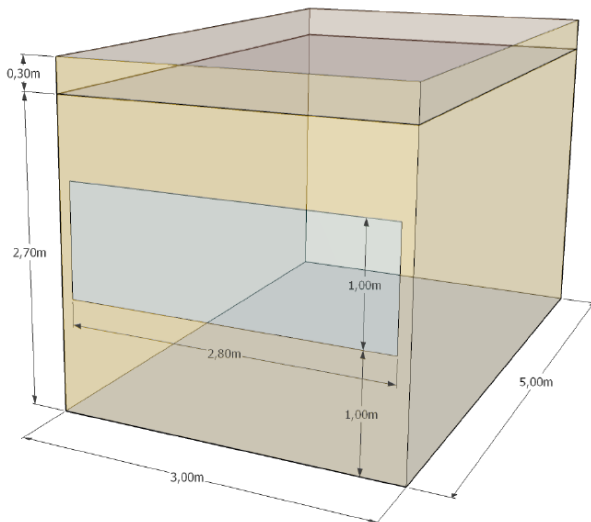


Fig. 2 Sketch of the office geometry (5m\*3m\*2.7m). The window is south-oriented

TABLE II  
WALL LAYOUTS

| Layout               | Material                                          | Thick. | Bnd.         |
|----------------------|---------------------------------------------------|--------|--------------|
| <b>Floor</b>         | Concrete                                          | 200mm  | $T_{ground}$ |
| <b>False ceiling</b> | Plasterboard Chilled ceiling                      | 50mm   | Adj.         |
| <b>Ceiling</b>       | Concrete                                          | 200mm  | Ext.         |
| <b>External wall</b> | Insulation                                        | 100mm  | Ext.         |
|                      | Concrete                                          | 200mm  |              |
|                      | Plasterboard                                      | 13mm   |              |
| <b>Partition</b>     | Insulation                                        | 50mm   | Adiab.       |
|                      | Plasterboard                                      | 13mm   |              |
| <b>Window</b>        | U-value = 1.27 W.m <sup>-2</sup> .K <sup>-1</sup> |        |              |

### C. Data Used

#### 1. Weather Data

Weather data for the location of Beirut were not available in TMY2 standard format. Weather data from Larnaca (Cyprus) are used instead. Larnaca has a similar location than Beirut, near the Mediterranean Sea. Fig. 3 displays the minimum, average and maximum temperature (Fig. 3 (a)), relative humidity (Fig. 3 (b)), direct solar radiation (Fig. 3 (c)) and dewpoint temperature (Fig. 3 (d)) for each month of a year. It also displays the first and last deciles to assess the data distribution.

#### 2. Ground Temperature

The ground temperature is a boundary condition of the simulation. Its value varies along the year with a sinusoidal

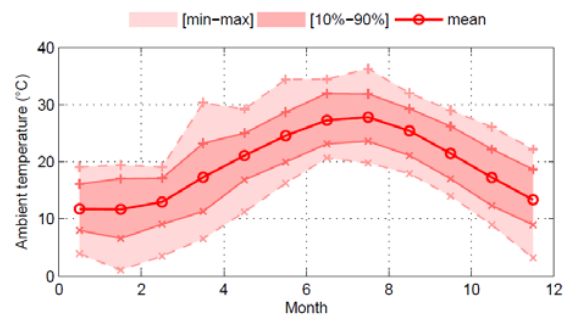
form as displayed in (1).

$$T_{ground} = 16 + 5 \sin\left(\frac{360(t - 5042)}{8760}\right) \quad (1)$$

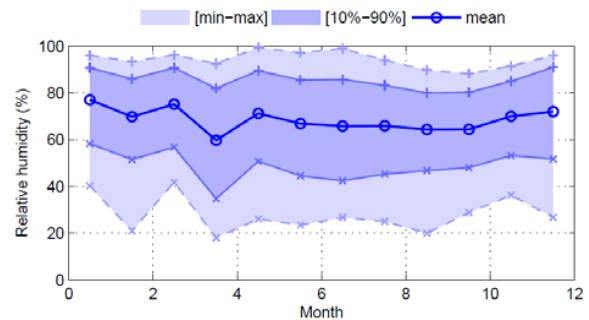
Equation (5) ensures an average ground temperature of 16 °C with an amplitude of variation of 10 °C. The maximum temperature is reached on July, 30<sup>th</sup>.

TABLE III  
MATERIAL PROPERTIES OF BUILDING FABRICS USED IN THE SIMULATION

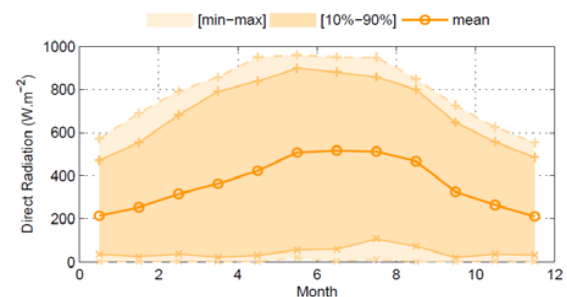
| Material            | Cond.<br>W.m.K <sup>-1</sup> | Capacity<br>kJ.kg <sup>-1</sup> .K <sup>-1</sup> | Density<br>kg.m <sup>-3</sup> |
|---------------------|------------------------------|--------------------------------------------------|-------------------------------|
| <b>Concrete</b>     | 1.17                         | 0.84                                             | 2000                          |
| <b>Insulation</b>   | 0.05                         | 0.84                                             | 50                            |
| <b>Plasterboard</b> | 0.16                         | 0.84                                             | 950                           |



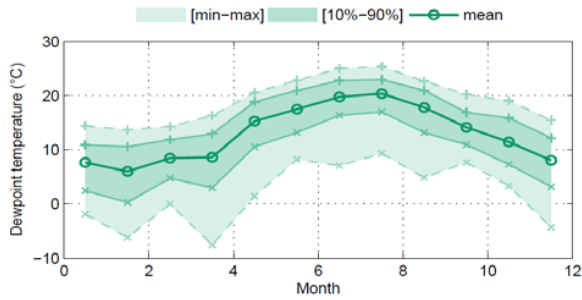
(a) Ambient temperature



(b) Relative humidity



(c) Direct solar radiation



(d) Dewpoint temperature

Fig. 3 Temperature, relative humidity, direct solar radiation profiles and dewpoint temperature profile and distribution for the weather data of Larnaca (Cyprus)

### 3. Comfort Indicators

Predictive mean vote (PMV) and predictive percentage of dissatisfied (PPD) are two indicators widely used in thermal comfort studies. They consist in a heat balance influenced by air temperature, radiant temperature, human metabolism, clothing insulation, air speed and relative humidity. They are calculated with a metabolic rate of 1.2 met, no external work (0 met), a relative velocity of 0.15 m. s<sup>-1</sup> and a clothing factor CLO that depends on the operative temperature  $T_{op}$  as defined in (2).

$$CLO = \begin{cases} 1 & , \text{if } T_{op} < 23^{\circ}\text{C} \\ 0.5 & , \text{if } T_{op} \geq 23^{\circ}\text{C} \end{cases} \quad (2)$$

### 4. Internal Gains

Internal gains due to human occupancy are accounted for. An occupancy schedule plans that the office space is occupied with two people for 10 hours a day (from 8:00 AM to 6:00 PM), 5/7, as shown in Fig. 4. Each person accounts for 70 W (half radiative and half convective) and for 50 gH<sub>2</sub>O.h<sup>-1</sup> (humidity).

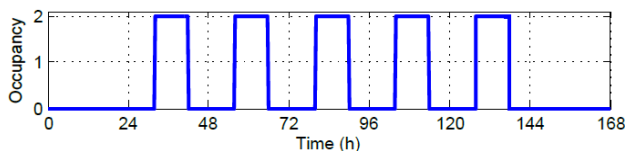


Fig. 4 Occupancy schedule

Lighting gains and electronic devices are not taken into account. Solar radiation is blinded by an internal shading of 50% as long as direct solar radiation are above a threshold value ( $I_T > 200 \text{ kJ. h}^{-1}$ ).

## III. RESULTS

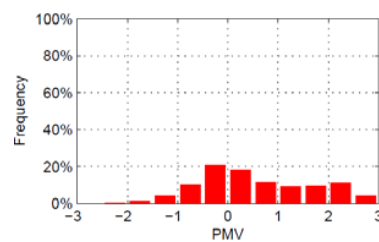
### A. Step 1: Free Evolution

The main objective of this first step is to estimate temperature and humidity values under a free evolution in order to highlight the need of a thermo-hygro regulation.

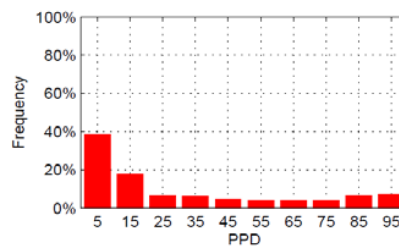
## 1. Results

### a) Comfort Indicators

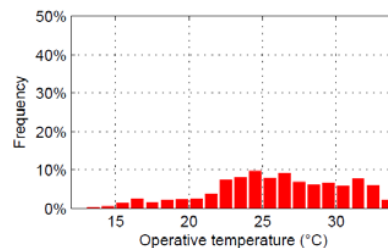
Comfort analysis shows a free evolution would lead to more than 10% of predictive dissatisfied for as often as 60% of the occupancy time (Fig. 5 (b)). The PMV distribution (Fig. 5 (a)) shows comfort issues are encountered on both too cold votes (negative values) and too hot votes (positive values). Negative values can easily be solved with a heating system (which does not lead to any humidity issues). Positive values call for a cooling system which justifies the scope of the project. Finally, operative temperature distribution goes from 11.2 °C to 33.9 °C on the whole year (on both occupancy and non occupancy periods). Extremum values are similar on occupation (Fig. 5 (c)) since there is no HVAC system to control the ambience.



(a) PMV distribution



(b) PPD distribution



(c) Operative temperature distribution

Fig. 5 PMV, PPD and operative temperature distributions (complete year) under free evolution and during occupation

### b) Humidity Distribution

Relative humidity varies from 17.1% to 91.2% (including non-occupancy periods). It should ideally remain in between 40% and 60% to satisfy comfort requirements. Fig. 6 displays humidity distribution ranked in descending order during occupancy hours.

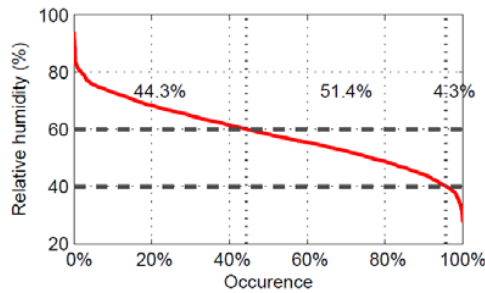


Fig. 6 Relative humidity distribution (during occupancy hours only) in case of a free evolution

### B. Step 2: Ideal HVAC System

Main objectives of the second step are to estimate the required cooling power and dehumidification rate in order to fulfill temperature and humidity set points in any case. The implementation of HVAC systems calls for the definition of some operating conditions.

#### 1. Operating Conditions

##### a) Ventilation System

The HVAC system (inlet fresh air) runs from 6:00 AM to 6:00 PM while occupancy schedule is from 8:00 AM to 6:00 PM with an air flowrate of 60 kg/h (which is in the scope with fresh air requirements for a two-occupant office). Two heat exchangers (heat recovery + heat sink) are used. They both have a constant effectiveness ( $\eta = 0.6$ ). The hot side inlet of the cooling heat exchanger is connected to inlet fresh air (from the heat recovery heat exchanger outlet). The cold side inlet is connected to a heat sink. The heat sink temperature  $T_{sink}$  is defined in (7). Equation (7) ensures an average temperature of 20 °C with an amplitude of variation of 8 °C over a year, and a maximum temperature reached on August, 20<sup>th</sup>.

$$T_{sink} = 20 + 4 \sin\left(\frac{360(t - 3380)}{8760}\right) \quad (3)$$

##### b) Temperature Control

Temperature control is achieved with ideal systems (during occupation). A heating load is provided to the room to maintain its temperature at 21 °C if necessary. A cooling load is provided to the room to maintain its temperature at 25 °C if necessary. A free temperature evolution occurs in between 21 °C and 25 °C, and with no condition during non-occupancy hours. These temperature points are chosen accordingly to the standard EN ISO 7730 in order to fulfill comfort requirements.

##### c) Humidity Control

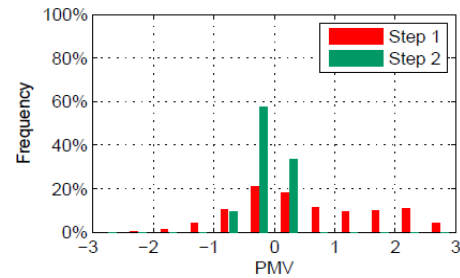
Humidity control is achieved with ideal humidification and dehumidification systems (during occupation). Humidity is provided to the room to maintain its temperature at 40% if necessary. Humidity is removed from the room to maintain its humidity at 60% if necessary. A free humidity evolution occurs in between 40% and 60%, and with no condition during non-occupancy hours. No humidity transfer occurs within the

walls. There is no buffer effect.

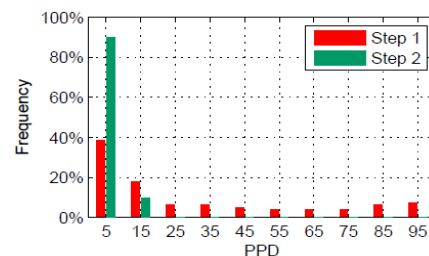
## 2. Results

### a) Comfort Indicators

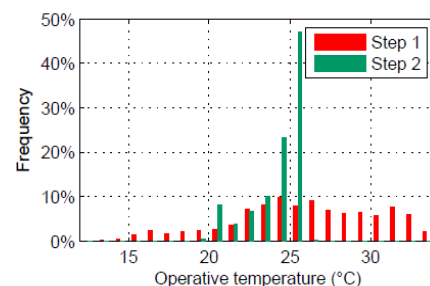
Fig. 7 shows that the PMV distribution is most of the time (90%) maintained in between 0.5 and +0.5 which ensures less than 10% of unsatisfied people. It also shows that the operative temperature distribution is maintained in between 19 °C and 27 °C.



(a) PMV distribution



(b) PPD distribution



(c) Operative temperature distribution

Fig. 7 PMV, PPD and operative temperature (complete year). Comparison between a free evolution (step 1) and an ideal HVAC system (step2), during occupation

The reason why the operative temperature remains above 25 °C (and below 27 °C) for about 43% of occupancy hours is because the control is achieved on the airnode temperature. Wall temperatures must be slightly higher than the airnode temperature which comes to higher operative temperature.

### b) Humidity Distribution

With an ideal humidification and dehumidification system, the relative humidity is maintained in between 40% and 60% during occupancy (as shown on Fig. 8 that compares the

relative humidity distribution in steps 1 and 2). During non-occupancy hours, the minimum relative humidity is 30.8%, and its maximum is 64.1%. These values are less critical than those of the free evolution analysis since humidity is controlled at regular intervals.

### c) Preliminary System Specifications

Results from this step with ideal HVAC systems show a dehumidification rate of  $49.2 \text{ g}_{\text{H}_2\text{O}} \text{ h}^{-1} \text{ m}^{-2}$  and a cooling power of  $49.7 \text{ Wm}^{-2}$  are reached with unlimited systems. Fig. 9 shows higher values are not necessarily occurring very often.

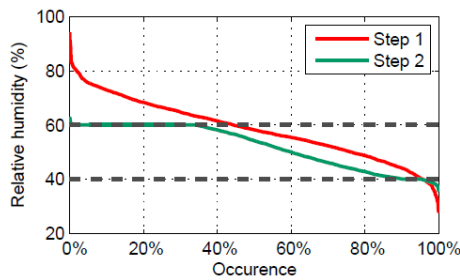


Fig. 8 Relative humidity and operative temperature distributions (during occupancy hours only). Comparison between a free evolution (step 1) and an ideal HVAC system (step2), during occupation

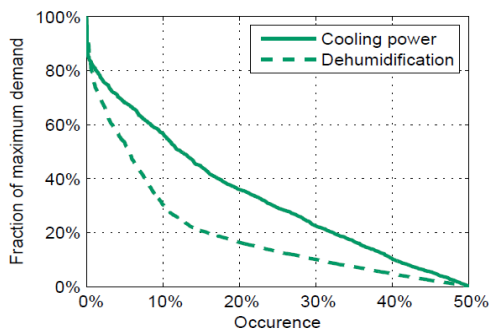


Fig. 9 Distributions of sorted cooling power and dehumidification rate with unlimited cooling and dehumidification systems

- It seems reasonable to size the system with lower requirements than maximum cooling power and maximum dehumidification rate. 85% of the maximum cooling power ( $\sim 42 \text{ Wm}^{-2}$ ) and 90% of the maximum dehumidification rate ( $\sim 45 \text{ g}_{\text{H}_2\text{O}} \text{ h}^{-1} \text{ m}^{-2}$ ) should be sufficient.

### C.Step 3: Realistic System

In this third step, a chilled ceiling is implemented. An analysis must be done, through a parametric study, to assess the variation of cooling performance, condensation risks and comfort issues with different sets of influencing parameters. A lot of parameters have a great influence on simulation results and could be selected for a parametric study. Stating that the main objective is to find the best operating conditions for the chilled ceiling, the inlet desiccant fluid temperature and the maximum flowrate are good candidates.

The implementation of the chilled ceiling requires the

definition of some operating conditions.

#### 1. Operating Conditions

##### a) Chilled Ceiling

In Trnsys, a chilled ceiling is directly defined in the Type 56 multizone tool (Trnbuild). Pipe spacing is set at 20 cm and pipe inside diameter is 2 cm. A direct contact between the chilled ceiling and the false ceiling is considered, so that heat transfer occurs through a conduction mechanism up to the ceiling surface which is in direct contact with the office space. In normalized conditions, a heat transfer coefficient of  $40 \text{ Wm}^{-2} \cdot \text{K}^{-1}$  is driving convection heat transfer between the ceiling surface and the office space air. Fig. 10 displays the chilled ceiling geometry to scale. The chilled ceiling can be controlled by its operating conditions, namely the temperature on the inlet fluid and the maximum flowrate allowed.

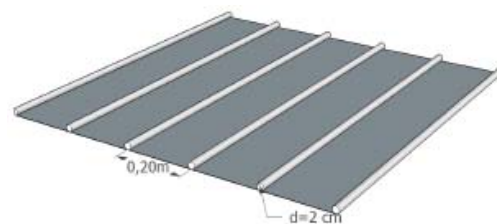


Fig. 10 Chilled ceiling geometry (pipe spacing and pipe diameter). Drawn to scale

The chilled ceiling inlet temperature is varied from  $14^\circ \text{C}$  to  $22^\circ \text{C}$  but remains constant for a given simulation. An inlet temperature higher than  $22^\circ \text{C}$  would provide too low cooling power regarding the set point temperature. An inlet temperature lower than  $14^\circ \text{C}$  would call for a low heat sink temperature: that sounds rather unlikely and inefficient. Please note that the blowing temperature of inlet fresh air remains constant ( $22^\circ \text{C}$ ) for all simulations, in order to solely outline the influence of the ceiling panel parameters on comfort and performance issues. A first iteration of parametric study has tested a wide range of maximum flow rate allowable. The final range, from  $50 \text{ L.h}^{-1}$  to  $1400 \text{ L.h}^{-1}$ , was selected to limit oversized cases. But, the chilled ceiling does not run continuously at its maximum flow rate. A schedule turns the chilled ceiling controller on and off. The control is achieved with a simple proportional controller which calculates the flow rate (in between 0 and the maximum flow rate) required to reach the setpoint operative temperature. The effective flow rate is then not necessarily equal to the maximum flow rate.

Fig. 11 displays the set of operating conditions considered in the parametric study. 45 different configurations have been tested.

##### b) Results Indicators

In order to compare each runs, it is necessary to define several scalar indicators. Some indicators aim at checking the system performance, others check comfort issues. They are evaluated for each of the 45 simulations and plotted in separated graphs in the remainder of this section.



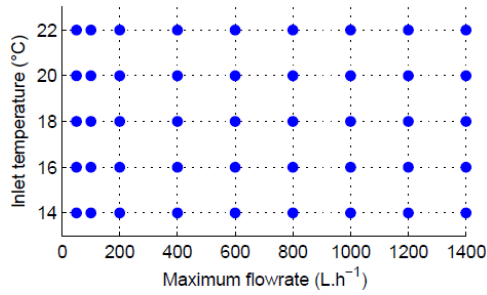


Fig. 11 Combinations of inlet temperature and maximum flowrate tested in the parametric study. One point is one simulation (total: 45 simulations)

*Performances indicators.* The following indicators are considered for system performance evaluation:

- maximum cooling power  $P_{cool,max}$
- mean cooling power  $\bar{P}_{cool}$
- maximum normalized flow rate  $\bar{m}_{cc,max}$
- mean normalized flow rate  $\bar{m}_{cc}/\bar{m}_{cc,max}$
- convective heat transfer coefficient  $h_{conv,mean}$  on the ceiling surface

*Comfort indicators.* The following indicators are calculated for comfort assessment:

- unsatisfying PMV values  $> 0.5$  (too warm) or  $< -0.5$  (too cold)
- unsatisfying operative temperatures  $T_{op}$ :
  - higher than  $25^\circ\text{C}$  (setpoint value  $T_{set}$ )
  - higher than  $26^\circ\text{C}$  ( $T_{op}-T_{set} > 1^\circ\text{C}$ )
  - higher than  $27^\circ\text{C}$  ( $T_{op}-T_{set} > 2^\circ\text{C}$ )

### c) Calculation Hypotheses

Different rules apply for the calculation of maximum and mean values. Calculations of maximum values are generally achieved upon the entire year, while calculations of mean values are achieved upon a specific and clearly specified time span (either the whole year, or for a single week in summer or in winter).

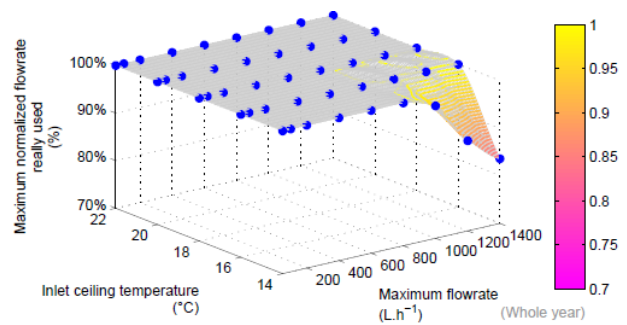
In the same way, comfort outputs are calculated only on occupancy hours (from 8:00 AM to 6:00 PM), while outputs regarding system behavior and performances are generally calculated upon running hours (i.e. when  $\dot{m}_{cc} > 0$ ).

## 2. Results from the Parametric Study

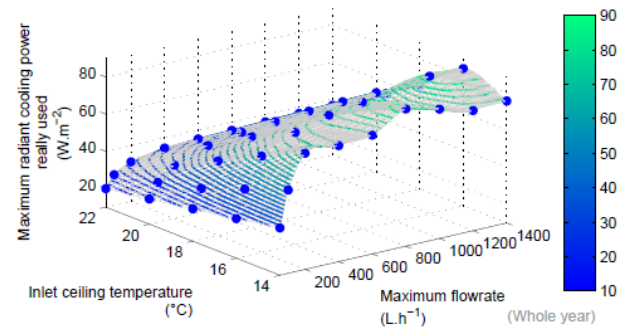
### a) Cooling Power and Inlet Water Flow Rate

- Maximum cooling power and maximum flow rate are interesting variables to assess if the system is oversized in a given configuration. Fig. 12 (a) displays the maximum normalized flow rate as a function of the inlet ceiling temperature and the maximum flow rate allowed. It shows that unless for combination of very high maximum flow rate (i.e.  $> 1000 \text{ L.h}^{-1}$ ) and very low inlet temperature (i.e.  $< 15^\circ\text{C}$ ), the maximum flow rate is always reached during the simulation. A similar observation is done on Fig.

12 (b), which displays the evolution of the maximum cooling power with different operating conditions. It is increasing with a flow rate increase and/or a temperature decrease up to a plateau at about  $80 \text{ W.m}^{-2}$ . This value is 60% higher than the design value of step 2 which sounds surprising. The chilled ceiling operating conditions are calculated on operative temperature while cooling needs of step 2 were calculated on airnode temperature. Moreover, the system inertia calls for higher power demand than with an ideal cooling system. Finally, these maximum values are to be lowered with regard to results of Fig. 9. It is then interesting to look at mean values. Fig. 14 displays evolutions of the mean flow rate and the mean cooling power for the entire year and for one summer week.



(a) Maximum normalized flow rate



(b) Maximum cooling power

Fig. 12 Maximum cooling power  $P_{cool,max}$  and normalized flow rate  $\bar{m}_{cc}$  as a function of inlet temperature  $T_{sink}$  and maximum flow rate

$\dot{m}_{max,cc}$  in the radiant cooling ceiling

For low flow rates ( $< 100 \text{ L.h}^{-1}$ ) or high inlet temperatures ( $> 20^\circ\text{C}$ ), the average flow rate is close to the maximum flow rate (Figs. 13 (a) and (b)). It shows that the cooling power is not sufficient and the system must run continuously. These operating conditions seem to lead to an undersizing of the system.

With less limiting flow rates and/or inlet temperatures, the mean cooling power is not so dependent on operating conditions (Figs. 13 (c) and (d)). The controller naturally reduces the average flow rate when the sink temperature is

low.

Fig. 13 (b) shows that it is not necessary to combine low sink temperatures ( $<18^\circ\text{C}$ ) with high flow rates ( $> 800 \text{ L.h}^{-1}$ ) or the system will be oversized. This corroborates observations of Fig. 12, but it notably extends the range of operating conditions where the system can be considered as oversized.

### c) Mean Convection Coefficient

Cooling load is transferred from the ceiling surface to the office space through radiation exchanges with the other room surfaces (calculated with view factors) and through convection. The convection coefficient used in the simulation is then of great importance to correctly assess system performances. This coefficient is calculated with:

$$h_{\text{conv}} = 7.2 \times (T_{\text{surf,cc}} - T_{\text{airnode}})^{0.31}$$

For all configurations, mean convection coefficient values are higher than  $2.5 \text{ W.m}^{-2}.\text{K}^{-1}$  and quickly reach a limiting value of  $3.5 \text{ W.m}^{-2}.\text{K}^{-1}$  when the inlet temperatures is lower than  $20^\circ\text{C}$  and the maximum flow rates is higher than  $200 \text{ L.h}^{-1}$ .

These values must be compared to CFD results, especially in the case of displacement ventilation.

## 3. Comfort Indicators

### a) Unsatisfying PMV Values

Fig. 14 shows that comfort values can globally be maintained within an acceptable range (less than 10% of PMV values over 0.5 or under -0.5) if operating conditions are chosen accordingly. Nevertheless, Fig. 14 (a) shows that the occurrence of PMV value lower than -0.5 is never lower than 5%. It is probably due to the heating setpoint temperature selected ( $21^\circ\text{C}$ ) that is in the low range of acceptable temperatures. Fig. 14 (a) also shows that a lack of comfort because of too cold environments can occur for chilled ceilings with high cooling powers. And yet, the heating systems is supposed ideal. It means that this lack of comfort occurs in summer and is due to an improper control of the chilled ceiling. Negative PMV values could probably be reduced with a better control strategy or more adaptive setpoint values.

Finally, Figs. 14 (a) and (b) show that a tradeoff must be found to reduce simultaneously low ( $<-0.5$ ) and high ( $> 0.5$ ) PMV values with constant operating conditions over the year.

### b) Occurrence of Unsatisfying Operative Temperatures

Fig. 15 is not easy to read since it overlaps three sets of data. It displays the occurrence of operative temperature above  $25^\circ\text{C}$  (which is the setpoint temperature), above  $26^\circ\text{C}$  and above  $27^\circ\text{C}$ .

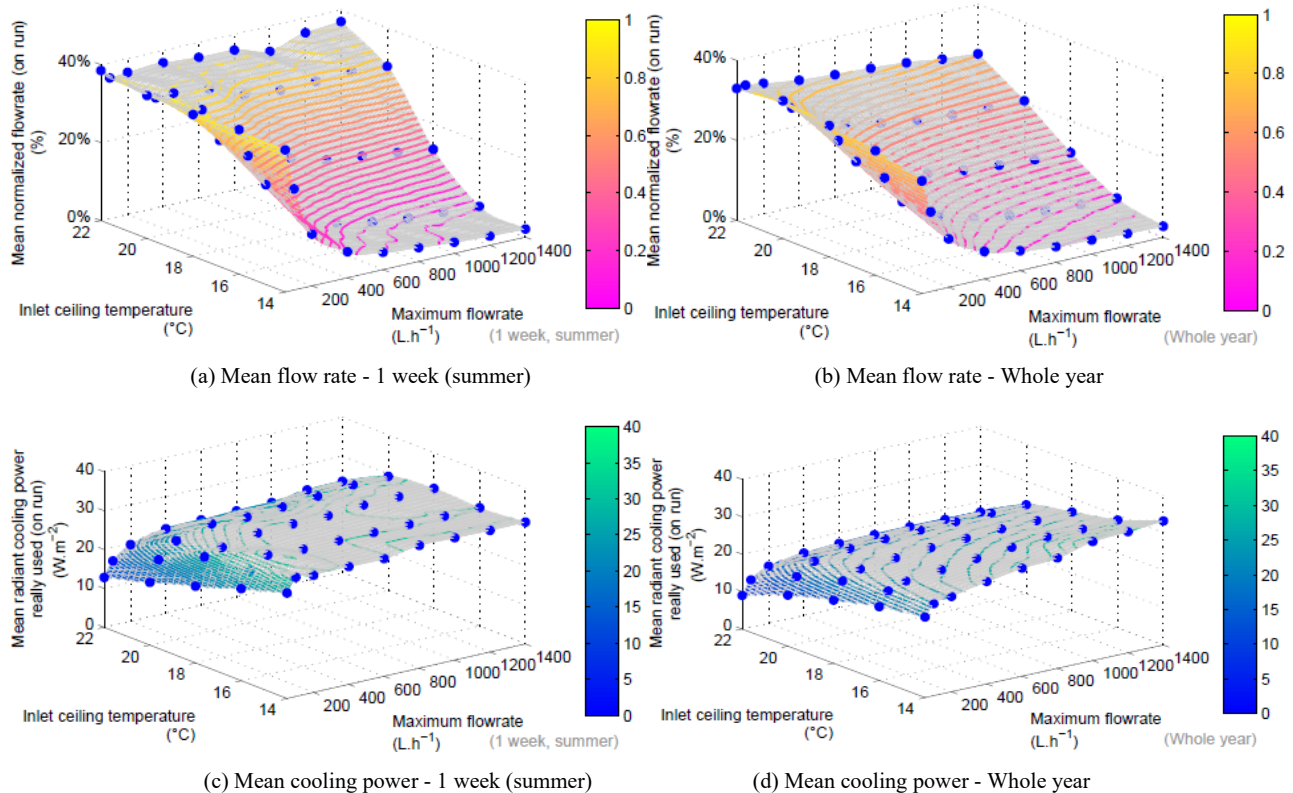


Fig. 13 Mean cooling power  $\bar{P}_{\text{cool}}$  and average normalized flow rate  $\bar{m}_{\text{cc}}^*$  as a function of inlet temperature  $T_{\text{sink}}$  and maximum flow rate

$$\dot{m}_{\text{max,cc}}$$



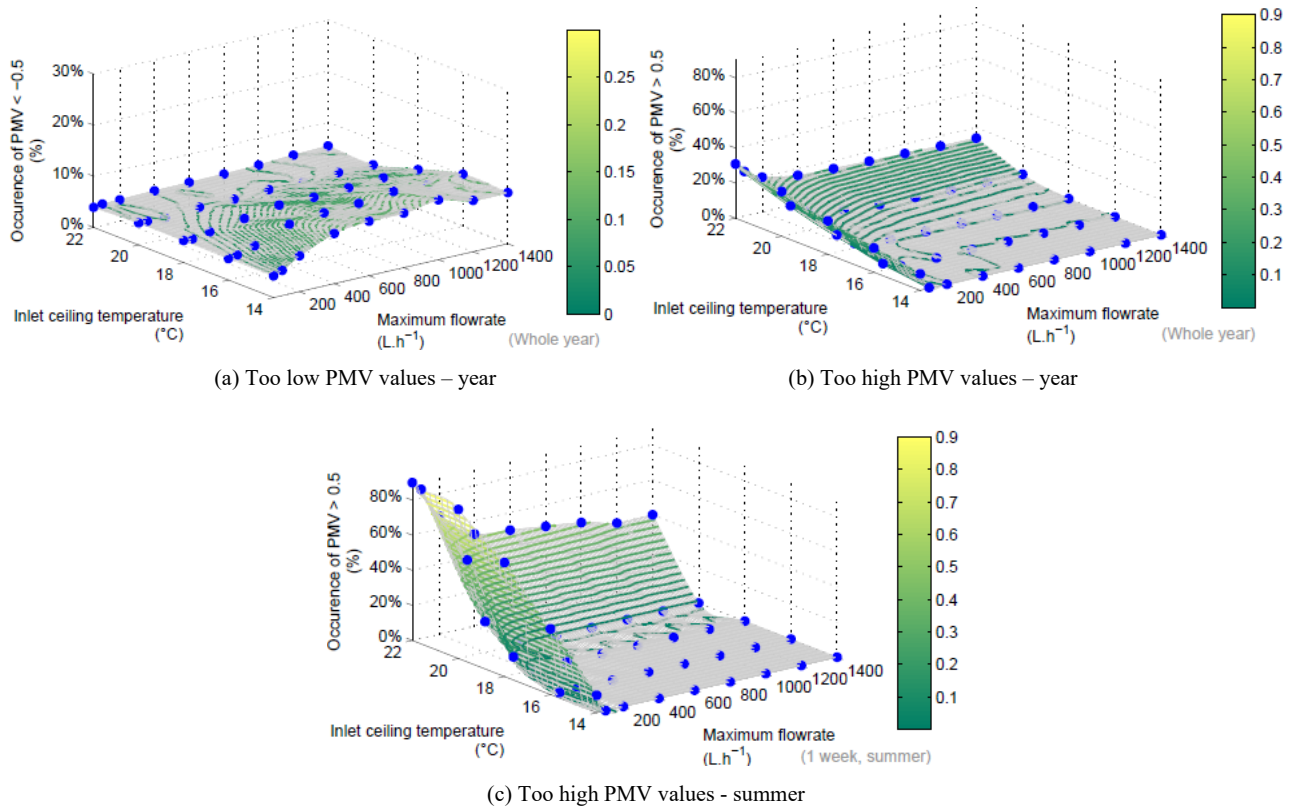


Fig. 14 Unsatisfying PMV values as a function of inlet temperature  $T_{sink}$  and maximum flow rate  $\dot{m}_{max,cc}$  in the radiant cooling ceiling

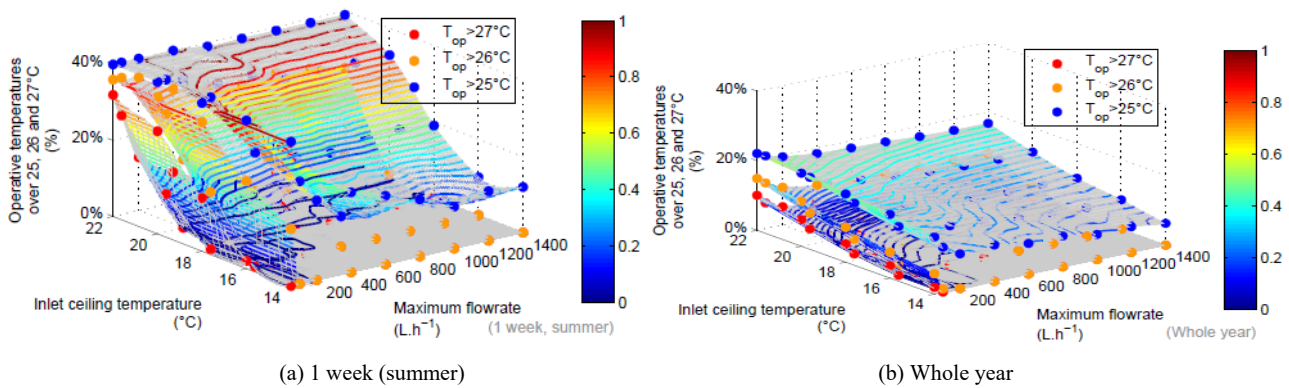


Fig. 15 Occurrence of unsatisfying operative temperatures (above 25, 26 and 27°C) as a function of inlet temperature  $T_{sink}$  and maximum flow rate  $\dot{m}_{max,cc}$  in the radiant cooling ceiling

If a temperature is above 27 °C it will also be above 26 and 25 °C. It is thus obvious that the first set ( $T_{op} > 27$  °C) has a greater occurrence than the second and the third one. The goal of these two charts is to check if the occurrence of unsatisfying operative temperatures remains in an acceptable range.

Fig. 15 (b) shows that, on the entire year (during occupancy hours), the operative temperature is higher than 25 °C for less than 20% of the time for all operating conditions under investigation. Occurrence of unsatisfying operative temperatures can be limited with any combination of inlet

temperature and maximum flow rate that enables a reasonably high cooling power (about 45W.m<sup>-2</sup>, which remains in the scope of the design values calculated in step 2).

#### c) Asymmetric Radiant Temperature

Radiant cooling can introduce large temperature differences between the surfaces of the room. If the difference is too large, it can lead to discomfort. Fig. 16 displays the difference between the ceiling temperature and the floor temperature ( $T_{surf,cc} - T_{floor}$ ).

Results show that the difference mainly depend on the inlet

temperature, very few on flow rate (unless for very low maximum flow rates, i.e.  $\dot{m}_{\max,cc} < 200 \text{ L.h}^{-1}$ ). This temperature difference is in between 5 °C and 8 °C, which should not generate more than 1% of dissatisfaction (as regard with EN ISO 7730). It is then not a concern for the present project.

#### d) Condensation Risks

Condensation risks are one of the main issues addressed by the Eranetmed Sol-Cool-Dry project. Fig. 17 displays the minimum difference between the ceiling surface temperature and the dewpoint temperature of the airnode ( $T_{\text{surf},cc} - T_{\text{dewpoint,airnode}}$ ). It shows the airnode dewpoint temperature is always at least 6 °C higher than the dewpoint temperature. Condensation risks seem to be limited. But, this is a nodal calculation which leads to simplified results, particularly because temperature or humidity stratification is not taken into account. It is also very important to underline that a dehumidification system ensures that the relative humidity of the room is never higher than 60%. This condition will not necessarily be met with the real system.

Finally, more unfavorable climate data can easily be found (higher temperatures and humidity ratios). Thus, these results must be used carefully.

#### 4. Conclusion of the Parametric Study

The parametric study has shown that it is necessary to choose the inlet ceiling temperature accordingly to the

maximum flow rate to prevent over/undersizing of the chilled ceiling.

The mean normalized flow rate is a good sizing variable. In the conditions of the present study, it should lie in between 50% and 60% of the maximum flow rate to meet both performance and comfort requirements.

Fig. 18 is a sizing chart derived from Fig. 13 (b). It shows there is an optimal combination between the inlet ceiling temperature and the maximum flow rate:

- Above 19 °C, a slight increase in the inlet ceiling temperature leads to a large increase in the maximum flow rate that is required to maintain an acceptable mean flow rate (e.g. 60 %).
- Under 200  $\text{L.h}^{-1}$ , a slight decrease in the maximum flow rate leads to a large decrease in the inlet ceiling temperature that is necessary to maintain an acceptable mean flow rate (e.g. 60 %).

A narrow range of combination of inlet ceiling temperature and maximum flow rate provides mean flow rate in between 40% and 70% of the maximum flow rate. The chilled ceiling is rapidly oversized or undersized. An inlet temperature  $T_{\text{sink}}$  of 18 °C and a maximum flow rate  $\dot{m}_{\max,cc}$  of 200  $\text{L.h}^{-1}$  are chosen for the remainder of the study, which compares results from the selected configuration of the third step with the results obtained in the first and second steps.

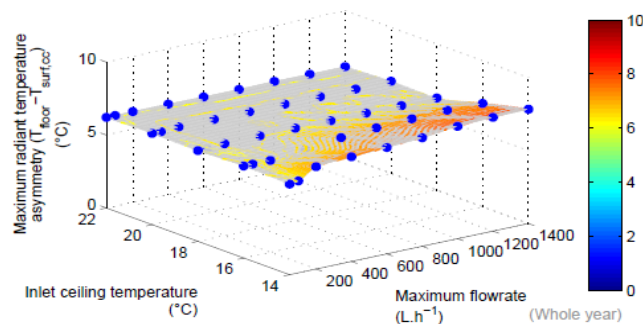


Fig. 16 Maximum asymmetric radiant temperature as a function of inlet temperature  $T_{\text{sink}}$  and maximum flow rate  $\dot{m}_{\max,cc}$  in the radiant cooling ceiling

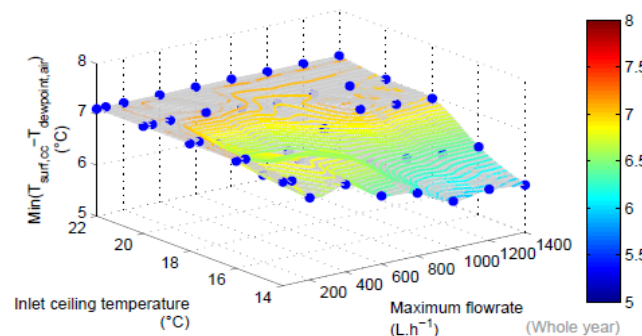


Fig. 17 Difference between ceiling surface temperature and airnode dewpoint temperature as a function of inlet temperature  $T_{\text{sink}}$  and maximum flow rate  $\dot{m}_{\max,cc}$  in the radiant cooling ceiling

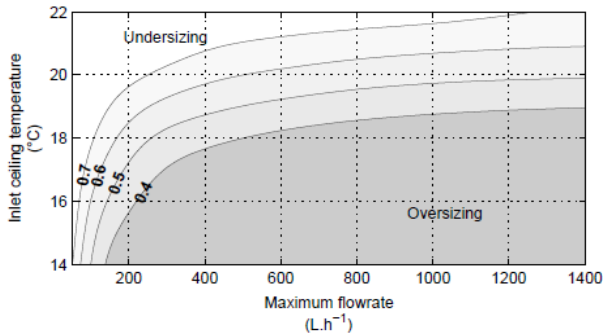
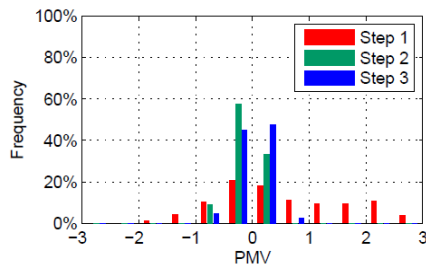
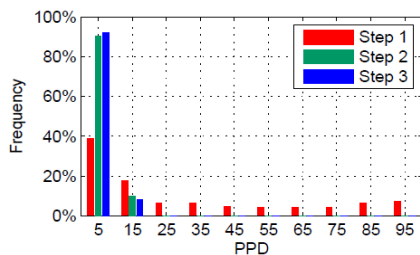


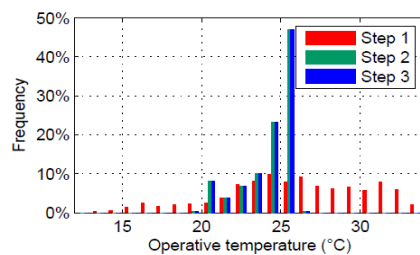
Fig. 18 Sizing chart derived from Fig. 13 (b)



(a) PMV distribution



(b) PPD distribution



(c) Operative temperature distribution

Fig. 19 PMV, PPD and operative temperature over a complete year (during occupancy hours only). Comparison between a free evolution (step 1), ideal HVAC system (step 2), and a chilled ceiling (step 3)

#### D. Step3: Single Case Analysis

##### 1. Comfort Indicators

With an inlet temperature of 18 °C and a maximum flow rate of 200 L.h<sup>-1</sup>, very good results are obtained on comfort. Fig. 19 (a) shows that the occurrence of PMV values in between -0.5 and +0.5 is slightly higher than what it was in the

second step.

It leads to 90% of satisfaction for about 90% of the time. In the remaining time (i.e. 10%), the percentage of satisfaction is in between 80% and 90% (Fig. 19 (b)).

Fig. 19 (c) displays the distribution of operative temperature. It shows the distribution of operative temperature is more diffuse than with the ideal HVAC system of step 2. Thus, the occurrence of operative temperature below the cooling setpoint temperature (25 °C) is increasing. But, there also are more operative temperatures above 26 °C (26 °C ≤ *Top* < 27 °C for about 8% of the occupancy hours, against 0% in the second step). In a general way, the use of a chilled ceiling is not detrimental to good comfort indicators.

##### 2. Humidity Distribution

On the entire year and including non-occupancy hours, the relative humidity reaches a minimum of 30.7% and a maximum of 64.8%. Fig. 20 displays the distribution of sorted humidity values (during occupancy hours). It shows that it remains most of the time in between 40% and 60% which is logical considering that an ideal dehumidification system is still in use.

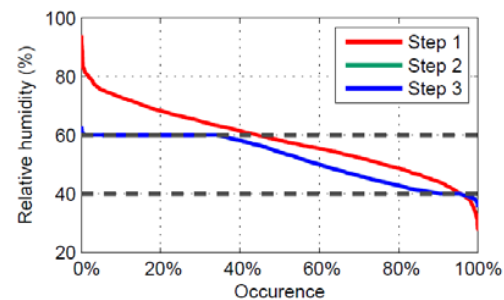


Fig. 20 Relative humidity distribution (occupancy hours only). Comparison between a free evolution (step 1), ideal system (step 2), and a chilled ceiling (step 3)

#### IV. CONCLUSION

This paper provides sizing information for a combined radiant cooling/dehumidification system. It assesses that an effective cooling power of 42W.m<sup>-2</sup> and a dehumidification rate of 45 g<sub>H2O</sub>.h<sup>-1</sup>.m<sup>-2</sup> should be sufficient to meet performance and comfort requirements.

The parametric study on the chilled ceiling behavior provided some assessments on the influence of operating conditions on comfort and performance issues. Fig. 18 provides a guideline to correlate the inlet fluid temperature and the maximum flow rate neither allowed in the chilled ceiling so that the system is neither over-sized nor under-sized. Nonetheless, the present study remains very simplified. Thus, a great care should be taken in the interpretation and in the use of these results. The simplified model developed here takes into account for:

- ✓ Heat and mass balances within the room:
  - Heat recovery and sink exchangers
  - Heat/cold loads to maintain setpoint
  - Vapor removal rate required to maintain humidity

setpoint

- ✓ Solar radiation and internal gains (sensible heat and humidity)

But it does not take into account for:

- ❖ Heat and vapor stratification
- ❖ Heat generation in the desiccant fluid and kinetic of absorption
- ❖ Desiccant fluid loop (constant inlet conditions instead of variable inlet conditions)

#### ACKNOWLEDGMENT

The work has been supported by the project « SOL-COOL-DRY » Sustainable Air Conditioning Using Desiccant Membrane System », ERA-NET MED 2015.

#### REFERENCES

- [1] G. J. Wood, "Membrane processes for heating, ventilation, and air conditioning," *Renewable and Sustainable Energy Reviews*, 2014, pp. 290-304.
- [2] A. Bakhtiar, F. Rokhman and C. K. HwaN, "Research on a Dehumidifier of Liquid Desiccant Type Solar Air Conditioning System for Full Year-round Use," *International Conference on Chemistry and Chemical Process, IPCBEE*, 2011 vol.10, Singapore.
- [3] A. Ameen and K. Mahmud, "Desiccant Dehumidification with Hydronic Radiant Cooling System for Air Conditioning Applications in Humid Tropical Climates", *ASHRAE*, 2005.
- [4] Y. Yin, X. Zhang, and Q. Chen, "Condensation risk in a room with high latent load and chilled ceiling panel and with air supplied from liquid desiccant system," *HVAC&R Research*, 2009, 315-327.
- [5] G. E Gaoming, A. H. Abdel-Salam, M. R. H. Abdel-Salam, R. W Besant and Carey J. Simonson, "Heat and mass transfer performance comparison between a direct-contact liquid desiccant packed bed and a liquid- to-air membrane energy exchanger for air dehumidification", *Science and Technology for the Built Environment* (2016) 00, 1–14.
- [6] A: Klein, S.A. et al, 2017, TRNSYS 18: A Transient System Simulation Program, Solar Energy Laboratory, University of Wisconsin, Madison, USA, <http://sel.me.wisc.edu/trnsys>.